

Measurement of inclusive prompt photon photoproduction at HERA

ZEUS Collaboration

Abstract

First inclusive measurements of isolated prompt photons in photoproduction at the HERA ep collider have been made with the ZEUS detector, using an integrated luminosity of 38.4 pb^{-1} . Cross sections are given as a function of the pseudorapidity and the transverse energy (η^γ , E_T^γ) of the photon, for $E_T^\gamma > 5 \text{ GeV}$ in the γp centre-of-mass energy range 134–285 GeV. Comparisons are made with predictions from Monte Carlo models having leading-logarithm parton showers, and with next-to-leading-order QCD calculations, using currently available parameterisations of the photon structure. For forward η^γ (proton direction) good agreement is found, but in the rear direction all predictions fall below the data.

The ZEUS Collaboration

J. Breitweg, S. Chekanov, M. Derrick, D. Krakauer, S. Magill, B. Musgrave, A. Pellegrino,
J. Repond, R. Stanek, R. Yoshida

Argonne National Laboratory, Argonne, IL, USA ^p

M.C.K. Mattingly

Andrews University, Berrien Springs, MI, USA

G. Abbiendi, F. Anselmo, P. Antonioli, G. Bari, M. Basile, L. Bellagamba, D. Boscherini¹,
A. Bruni, G. Bruni, G. Cara Romeo, G. Castellini², L. Cifarelli³, F. Cindolo, A. Contin,
N. Coppola, M. Corradi, S. De Pasquale, P. Giusti, G. Iacobucci, G. Laurenti, G. Levi,
A. Margotti, T. Massam, R. Nania, F. Palmonari, A. Pesci, A. Polini, G. Sartorelli,
Y. Zamora Garcia⁴, A. Zichichi

University and INFN Bologna, Bologna, Italy ^f

C. Amelung, A. Bornheim, I. Brock, K. Coböken, J. Crittenden, R. Deffner, H. Hartmann,
K. Heinloth, E. Hilger, H.-P. Jakob, A. Kappes, U.F. Katz, R. Kerger, E. Paul,
J. Rautenberg⁵, H. Schnurbusch,

A. Stifutkin, J. Tandler, K.Ch. Voss, A. Weber, H. Wieber

Physikalisches Institut der Universität Bonn, Bonn, Germany ^c

D.S. Bailey, O. Barret, N.H. Brook⁶, B. Foster⁷, G.P. Heath, H.F. Heath, J.D. McFall,
D. Piccioni, E. Rodrigues, J. Scott, R.J. Tapper

H.H. Wills Physics Laboratory, University of Bristol, Bristol, U.K. ^o

M. Capua, A. Mastroberardino, M. Schioppa, G. Susinno

Calabria University, Physics Dept. and INFN, Cosenza, Italy ^f

H.Y. Jeoung, J.Y. Kim, J.H. Lee, I.T. Lim, K.J. Ma, M.Y. Pac⁸

Chonnam National University, Kwangju, Korea ^h

A. Caldwell, W. Liu, X. Liu, B. Mellado, R. Sacchi, S. Sampson, F. Sciulli

Columbia University, Nevis Labs., Irvington on Hudson, N.Y., USA ^q

J. Chwastowski, A. Eskreys, J. Figiel, K. Klimek, K. Olkiewicz, M.B. Przybycień, P. Stopa,
L. Zawiejski

Inst. of Nuclear Physics, Cracow, Poland ^j

L. Adamczyk⁹, B. Bednarek, K. Jeleń, D. Kisielewska, A.M. Kowal, T. Kowalski, M. Przybycień,

E. Rulikowska-Zarębska, L. Suszycki, J. Zajac

Faculty of Physics and Nuclear Techniques, Academy of Mining and Metallurgy, Cracow, Poland ^j

A. Kotański

Jagellonian Univ., Dept. of Physics, Cracow, Poland ^k

L.A.T. Bauerdick, U. Behrens, J.K. Bienlein, C. Burgard¹⁰, K. Desler, G. Drews, A. Fox-Murphy, U. Fricke, F. Goebel, P. Göttlicher, R. Graciani, T. Haas, W. Hain, G.F. Hartner, D. Hasell¹¹, K. Hebbel, K.F. Johnson¹², M. Kasemann¹³, W. Koch, U. Kötz, H. Kowalski, L. Lindemann¹⁴, B. Löhr, M. Martínez, M. Milite, T. Monteiro¹⁵, M. Moritz, D. Notz, F. Pelucchi, M.C. Petrucci, K. Piotrkowski¹⁵, M. Rohde, P.R.B. Saull, A.A. Savin, U. Schneekloth, F. Selonke, M. Sievers, S. Stonjek, E. Tassi, G. Wolf, U. Wollmer, C. Youngman, W. Zeuner
Deutsches Elektronen-Synchrotron DESY, Hamburg, Germany

C. Coldewey, H.J. Grabosch, A. Lopez-Duran Viani, A. Meyer, S. Schlenstedt, P.B. Straub
DESY Zeuthen, Zeuthen, Germany

G. Barbagli, E. Gallo, P. Pelfer
University and INFN, Florence, Italy^f

G. Maccarrone, L. Votano
INFN, Laboratori Nazionali di Frascati, Frascati, Italy^f

A. Bamberger, S. Eisenhardt¹⁶, P. Markun, H. Raach, S. Wölflé
Fakultät für Physik der Universität Freiburg i.Br., Freiburg i.Br., Germany^c

P.J. Bussey, A.T. Doyle, S.W. Lee, N. Macdonald, G.J. McCance, D.H. Saxon, L.E. Sinclair,
I.O. Skillicorn, R. Waugh
Dept. of Physics and Astronomy, University of Glasgow, Glasgow, U.K.^o

I. Bohnet, N. Gendner, U. Holm, A. Meyer-Larsen, H. Salehi, K. Wick
Hamburg University, I. Institute of Exp. Physics, Hamburg, Germany^c

A. Garfagnini, I. Gialas¹⁷, L.K. Gladilin¹⁸, D. Kçira¹⁹, R. Klanner, E. Lohrmann, G. Poelz, F. Zetsche
Hamburg University, II. Institute of Exp. Physics, Hamburg, Germany^c

R. Goncalo, K.R. Long, D.B. Miller, A.D. Tapper, R. Walker
Imperial College London, High Energy Nuclear Physics Group, London, U.K.^o

U. Mallik, S.M. Wang
University of Iowa, Physics and Astronomy Dept., Iowa City, USA^p

P. Cloth, D. Filges
Forschungszentrum Jülich, Institut für Kernphysik, Jülich, Germany

T. Ishii, M. Kuze, K. Nagano, K. Tokushuku²⁰, S. Yamada, Y. Yamazaki
Institute of Particle and Nuclear Studies, KEK, Tsukuba, Japan^g

S.H. Ahn, S.H. An, S.J. Hong, S.B. Lee, S.W. Nam²¹, S.K. Park
Korea University, Seoul, Korea^h

H. Lim, I.H. Park, D. Son
Kyungpook National University, Taegu, Korea^h

F. Barreiro, G. García, C. Glasman²², O. Gonzalez, L. Labarga, J. del Peso, I. Redondo²³, J. Terrón

Univer. Autónoma Madrid, Depto de Física Teórica, Madrid, Spainⁿ

M. Barbi, F. Corriveau, D.S. Hanna, A. Ochs, S. Padhi, M. Riveline, D.G. Stairs, M. Wing
McGill University, Dept. of Physics, Montréal, Québec, Canada^{a, b}

T. Tsurugai

Meiji Gakuin University, Faculty of General Education, Yokohama, Japan

V. Bashkirov²⁴, B.A. Dolgoshein

Moscow Engineering Physics Institute, Moscow, Russia^l

G.L. Bashindzhagyan, P.F. Ermolov, Yu.A. Golubkov, L.A. Khein, N.A. Korotkova, I.A. Korzhavina, V.A. Kuzmin, O.Yu. Lukina, A.S. Proskuryakov, L.M. Shcheglova, A.N. Solomin, S.A. Zotkin

Moscow State University, Institute of Nuclear Physics, Moscow, Russia^m

C. Bokel, M. Botje, N. Brümmer, J. Engelen, E. Koffeman, P. Kooijman, A. van Sighem, H. Tiecke, N. Tuning, J.J. Velthuis, W. Verkerke, J. Vossebeld, L. Wiggers, E. de Wolf
NIKHEF and University of Amsterdam, Amsterdam, Netherlandsⁱ

B. Bylsma, L.S. Durkin, J. Gilmore, C.M. Ginsburg, C.L. Kim, T.Y. Ling, P. Nylander²⁵
Ohio State University, Physics Department, Columbus, Ohio, USA^p

S. Boogert, A.M. Cooper-Sarkar, R.C.E. Devenish, J. Große-Knetter²⁶, T. Matsushita, O. Ruske,

M.R. Sutton, R. Walczak

Department of Physics, University of Oxford, Oxford U.K.^o

A. Bertolin, R. Brugnera, R. Carlin, F. Dal Corso, S. Dondana, U. Dosselli, S. Dusini, S. Limentani, M. Morandin, M. Posocco, L. Stanco, R. Stroili, C. Voci

Dipartimento di Fisica dell'Università and INFN, Padova, Italy^f

L. Iannotti²⁷, B.Y. Oh, J.R. Okrasinski, W.S. Toothacker, J.J. Whitmore

Pennsylvania State University, Dept. of Physics, University Park, PA, USA^q

Y. Iga

Polytechnic University, Sagamihara, Japan^g

G. D'Agostini, G. Marini, A. Nigro

Dipartimento di Fisica, Univ. 'La Sapienza' and INFN, Rome, Italy^f

C. Cormack, J.C. Hart, N.A. McCubbin, T.P. Shah

Rutherford Appleton Laboratory, Chilton, Didcot, Oxon, U.K.^o

D. Epperson, C. Heusch, H.F.-W. Sadrozinski, A. Seiden, R. Wichmann, D.C. Williams

University of California, Santa Cruz, CA, USA^p

N. Pavel

Fachbereich Physik der Universität-Gesamthochschule Siegen, Germany^c

H. Abramowicz²⁸, S. Dagan²⁹, S. Kananov²⁹, A. Kreisel, A. Levy²⁹
*Raymond and Beverly Sackler Faculty of Exact Sciences, School of Physics, Tel-Aviv
University,
Tel-Aviv, Israel*^e

T. Abe, T. Fusayasu, K. Umemori, T. Yamashita
Department of Physics, University of Tokyo, Tokyo, Japan^g

R. Hamatsu, T. Hirose, M. Inuzuka, S. Kitamura³⁰, T. Nishimura
Tokyo Metropolitan University, Dept. of Physics, Tokyo, Japan^g

M. Arneodo³¹, N. Cartiglia, R. Cirio, M. Costa, M.I. Ferrero, S. Maselli, V. Monaco,
C. Peroni, M. Ruspa, A. Solano, A. Staiano
Università di Torino, Dipartimento di Fisica Sperimentale and INFN, Torino, Italy^f

M. Dardo
II Faculty of Sciences, Torino University and INFN - Alessandria, Italy^f

D.C. Bailey, C.-P. Fagerstroem, R. Galea, T. Koop, G.M. Levman, J.F. Martin, R.S. Orr,
S. Polenz, A. Sabetfakhri, D. Simmons
University of Toronto, Dept. of Physics, Toronto, Ont., Canada^a

J.M. Butterworth, C.D. Catterall, M.E. Hayes, E.A. Heaphy, T.W. Jones, J.B. Lane,
B.J. West
University College London, Physics and Astronomy Dept., London, U.K.^o

J. Ciborowski, R. Ciesielski, G. Grzelak, R.J. Nowak, J.M. Pawlak, R. Pawlak, B. Smalska,
T. Tymieniecka, A.K. Wróblewski, J.A. Zakrzewski, A.F. Żarnecki
Warsaw University, Institute of Experimental Physics, Warsaw, Poland^j

M. Adamus, T. Gadaj
Institute for Nuclear Studies, Warsaw, Poland^j

O. Deppe, Y. Eisenberg²⁹, D. Hochman, U. Karshon²⁹
Weizmann Institute, Department of Particle Physics, Rehovot, Israel^d

W.F. Badgett, D. Chapin, R. Cross, C. Foudas, S. Mattingly, D.D. Reeder, W.H. Smith,
A. Vaiciulis³², T. Wildschek, M. Wodarczyk
University of Wisconsin, Dept. of Physics, Madison, WI, USA^p

A. Deshpande, S. Dhawan, V.W. Hughes
Yale University, Department of Physics, New Haven, CT, USA^p

S. Bhadra, J.E. Cole, W.R. Frisken, R. Hall-Wilton, M. Khakzad, S. Menary, W.B. Schmidke
York University, Dept. of Physics, Toronto, Ont., Canada^a

- ¹ now visiting scientist at DESY
- ² also at IROE Florence, Italy
- ³ now at Univ. of Salerno and INFN Napoli, Italy
- ⁴ supported by Worldlab, Lausanne, Switzerland
- ⁵ drafted to the German military service
- ⁶ PPARC Advanced fellow
- ⁷ also at University of Hamburg, Alexander von Humboldt Research Award
- ⁸ now at Dongshin University, Naju, Korea
- ⁹ supported by the Polish State Committee for Scientific Research, grant No. 2P03B14912
- ¹⁰ now at Barclays Capital PLC, London
- ¹¹ now at Massachusetts Institute of Technology, Cambridge, MA, USA
- ¹² visitor from Florida State University
- ¹³ now at Fermilab, Batavia, IL, USA
- ¹⁴ now at SAP A.G., Walldorf, Germany
- ¹⁵ now at CERN
- ¹⁶ now at University of Edinburgh, Edinburgh, U.K.
- ¹⁷ visitor of Univ. of Crete, Greece, partially supported by DAAD, Bonn - Kz. A/98/16764
- ¹⁸ on leave from MSU, supported by the GIF, contract I-0444-176.07/95
- ¹⁹ supported by DAAD, Bonn - Kz. A/98/12712
- ²⁰ also at University of Tokyo
- ²¹ now at Wayne State University, Detroit
- ²² supported by an EC fellowship number ERBFMBICT 972523
- ²³ supported by the Comunidad Autonoma de Madrid
- ²⁴ now at Loma Linda University, Loma Linda, CA, USA
- ²⁵ now at Hi Techniques, Inc., Madison, WI, USA
- ²⁶ supported by the Feodor Lynen Program of the Alexander von Humboldt foundation
- ²⁷ partly supported by Tel Aviv University
- ²⁸ an Alexander von Humboldt Fellow at University of Hamburg
- ²⁹ supported by a MINERVA Fellowship
- ³⁰ present address: Tokyo Metropolitan University of Health Sciences, Tokyo 116-8551, Japan
- ³¹ now also at Università del Piemonte Orientale, I-28100 Novara, Italy
- ³² now at University of Rochester, Rochester, NY, USA

- ^a supported by the Natural Sciences and Engineering Research Council of Canada (NSERC)
- ^b supported by the FCAR of Québec, Canada
- ^c supported by the German Federal Ministry for Education and Science, Research and Technology (BMBF), under contract numbers 057BN19P, 057FR19P, 057HH19P, 057HH29P, 057SI75I
- ^d supported by the MINERVA Gesellschaft für Forschung GmbH, the German Israeli Foundation, and by the Israel Ministry of Science
- ^e supported by the German-Israeli Foundation, the Israel Science Foundation, the U.S.-Israel Binational Science Foundation, and by the Israel Ministry of Science
- ^f supported by the Italian National Institute for Nuclear Physics (INFN)
- ^g supported by the Japanese Ministry of Education, Science and Culture (the Monbusho) and its grants for Scientific Research
- ^h supported by the Korean Ministry of Education and Korea Science and Engineering Foundation
- ⁱ supported by the Netherlands Foundation for Research on Matter (FOM)
- ^j supported by the Polish State Committee for Scientific Research, grant No. 115/E-343/SPUB/P03/154/98, 2P03B03216, 2P03B04616, 2P03B10412, 2P03B03517, and by the German Federal Ministry of Education and Science, Research and Technology (BMBF)
- ^k supported by the Polish State Committee for Scientific Research (grant No. 2P03B08614 and 2P03B06116)
- ^l partially supported by the German Federal Ministry for Education and Science, Research and Technology (BMBF)
- ^m supported by the Fund for Fundamental Research of Russian Ministry for Science and Education and by the German Federal Ministry for Education and Science, Research and Technology (BMBF)
- ⁿ supported by the Spanish Ministry of Education and Science through funds provided by CICYT
- ^o supported by the Particle Physics and Astronomy Research Council
- ^p supported by the US Department of Energy
- ^q supported by the US National Science Foundation

1 Introduction

One of the primary aims of photoproduction measurements in ep collisions at HERA is the elucidation of the hadronic behaviour of the photon. The measurement of jets at high transverse energy has provided much information in this area [1, 2]. In the study of inclusive jets, next-to-leading order (NLO) QCD calculations are able to describe the experimental data over a wide range of kinematic conditions, although the agreement is dependent on the jet algorithm [3]. However, significant discrepancies between data and NLO theories are found in dijet measurements [4]. A further means to study photoproduction is provided by final states with an isolated high-transverse-energy photon. These have the particular merit that the photon may emerge directly from the hard QCD subprocess (“prompt” photons), and also can be investigated without the hadronisation corrections needed in the case of quarks or gluons. In a previous measurement by ZEUS at HERA [5], it was shown that prompt photons, accompanied by balancing jets, are produced at the expected level in photoproduction and with the expected event characteristics. This work is extended in the present paper through the use of a much larger event sample taken in 1996-97, corresponding to an integrated ep luminosity of 38.4 pb^{-1} . This allows a measurement of inclusive prompt photon distributions as a function of pseudorapidity η^γ and transverse energy E_T^γ of the photon, and a comparison with LO and NLO QCD predictions.

2 Apparatus and trigger

During 1996-97, HERA collided positrons with energy $E_e = 27.5 \text{ GeV}$ with protons of energy $E_p = 820 \text{ GeV}$. The luminosity was measured by means of the bremsstrahlung process $ep \rightarrow e\gamma p$.

A description of the ZEUS apparatus and luminosity monitor is given elsewhere [6]. Of particular importance in the present work are the uranium calorimeter (CAL) and the central tracking detector (CTD).

The CAL [7] has an angular coverage of 99.7% of 4π and is divided into three parts (FCAL, BCAL, RCAL), covering the forward (proton direction), central and rear angular ranges, respectively. Each part consists of towers longitudinally subdivided into electromagnetic (EMC) and hadronic (HAC) cells. The electromagnetic section of the BCAL (BEMC) consists of cells of $\sim 20 \text{ cm}$ length azimuthally and mean width 5.45 cm in the Z direction¹, at a mean radius of $\sim 1.3 \text{ m}$ from the beam line. These cells have a projective geometry as viewed from the interaction point. The profile of the electromagnetic signals observed in clusters of cells in the BEMC provides a partial discrimination between those originating from photons or positrons, and those originating from neutral meson decays.

The CTD [8] is a cylindrical drift chamber situated inside a superconducting solenoid which produces a 1.43 T field. Using the tracking information from the CTD, the vertex of an event can be reconstructed with a resolution of 0.4 cm in Z and 0.1 cm in X, Y . In

¹ The ZEUS coordinate system is right-handed with positive- Z in the proton beam direction and an upward-pointing Y axis. The nominal interaction point is at $X = Y = Z = 0$.

this analysis, the CTD tracks are used to reconstruct the event vertex, and also in the selection criteria for high- E_T photons.

The ZEUS detector uses a three-level trigger system, of which the first- and second-level triggers used in this analysis have been described previously [5]. The third-level trigger made use of a standard ZEUS electron finding algorithm [9] to select events with an electromagnetic cluster of transverse energy $E_T > 4$ GeV in the BCAL, with no further tracking requirements at this stage. These events represent the basic sample of prompt photon event candidates.

3 Event selection

The offline analysis was based on previously developed methods [5]. An algorithm for finding electromagnetic clusters was applied to the data, and events were retained for final analysis if a photon candidate with $E_T > 5$ GeV was found in the BCAL. A photon candidate was rejected if a CTD track, as measured at the vertex, pointed to it within 0.3 radians; this removed almost all high- E_T positrons and electrons, including the majority of those that underwent hard radiation. The BCAL requirement restricts the photon candidates to the approximate pseudorapidity² range $-0.75 < \eta^\gamma < 1.0$.

Events with an identified deep inelastic scattered (DIS) positron in addition to the BCAL photon candidate were removed, thus restricting the acceptance to incident photons of virtuality $Q^2 \lesssim 1$ GeV². The quantity $y^{meas} = \sum(E - p_z)/2E_e$ was calculated, where the sum is over all calorimeter cells, E is the energy deposited in the cell, and $p_z = E \cos \theta$. When the outgoing positron is not detected in the CAL, y^{meas} is a measure of $y = E_{\gamma, in}/E_e$, where $E_{\gamma, in}$ is the energy of the incident photon. If the outgoing positron is detected in the CAL, $y^{meas} \approx 1$. A requirement of $0.15 < y^{meas} < 0.7$ was imposed; the lower cut removed some residual proton-gas backgrounds while the upper cut removed remaining DIS events, including any with a photon candidate that was actually a misidentified DIS positron. Wide-angle Compton scattering events ($ep \rightarrow e\gamma p$) were also excluded by this cut. This range of accepted y^{meas} values corresponds approximately to the true y range $0.2 < y < 0.9$.

An isolation cone was imposed around the photon candidate: within a cone of unit radius in (η, ϕ) , the total E_T from other particles was required not to exceed $0.1E_T^\gamma$. This was calculated by summing the E_T in each calorimeter cell within the isolation cone. Further contributions were included from charged tracks which originated within the isolation cone but curved out of it; the small number of tracks which curved into the isolation cone were ignored. The isolation condition much reduces the dijet background by removing a large majority of the events where the photon candidate is closely associated with a jet and is therefore either hadronic (e.g. a π^0) or else a photon radiated within a jet. In particular, the isolation condition removes most dijet events in which a photon is radiated from a final-state quark. Approximately 6000 events with $E_T^\gamma > 5$ GeV remained after the above cuts.

² All kinematic quantities are given in the laboratory frame. Pseudorapidity η is defined as $-\ln \tan(\theta/2)$, where θ is the polar angle relative to the Z direction, measured from the Z position of the event vertex.

Studies based on the single-particle Monte Carlo samples showed that the photon energy measured in the CAL was on average less than the true value, owing to dead material in front of the CAL. To compensate for this, an energy correction, typically 0.2 GeV, was added.

4 Monte Carlo simulations

In describing the hard interaction of photons of low virtuality with protons, two major classes of diagram are important. In one of these the photon couples in a pointlike way to a $q\bar{q}$ pair, while in the other the photon interacts via an intermediate hadronic state, which provides quarks and gluons which then take part in the hard QCD subprocesses. At leading order (LO) in QCD, the pointlike and hadronic diagrams are distinct and are commonly referred to as direct and resolved processes, respectively.

In the present analysis, three types of Monte Carlo samples were employed to simulate: (1) the LO QCD prompt photon processes, (2) dijet processes in which an outgoing quark radiated a hard photon (radiative events), and (3) single particles (γ , π^0 , η) at high E_T . All generated events were passed through a full GEANT-based simulation [10] of the ZEUS detector.

The PYTHIA 5.7 [11] and HERWIG 5.9 [12] Monte Carlo generators were both used to simulate the direct and resolved prompt photon processes. These generators include LO QCD subprocesses and higher-order processes modelled by initial- and final-state parton showers. The parton density function (pdf) sets used were MRSA [13] for the proton, and GRV(LO) [14] for the photon. The minimum p_T of the hard scatter was set to 2.5 GeV. No multi-parton interactions were implemented in the resolved samples. The radiative event samples were likewise produced using direct and resolved photoproduction generators within PYTHIA and HERWIG.

In modelling the overall photoproduction process, the event samples produced for the separate direct, resolved and radiative processes were combined in proportion to their total cross sections as calculated by the generators. A major difference between PYTHIA and HERWIG is the smaller radiative contribution in the HERWIG model.

Three Monte Carlo single-particle data sets were generated, comprising large samples of γ , π^0 and η . The single particles were generated uniformly over the acceptance of the BCAL and with a flat E_T distribution between 3 and 20 GeV; E_T -dependent exponential weighting functions were subsequently applied to reproduce the observed distributions. These samples were used in separating the signal from the background using shower shapes.

5 Evaluation of the photon signal

Signals in the BEMC that do not arise from charged particles are predominantly due to photons, π^0 mesons and η mesons. A large fraction of these mesons decay into multiphoton

final states, the π^0 through its 2γ channel and the η through its 2γ and $3\pi^0$ channels. For π^0 , η produced with E_T greater than a few GeV, the photons from the decays are separated in the BEMC by distances comparable to the BEMC cell width in Z . Therefore the discrimination between photons and neutral mesons was performed on the basis of cluster-shape characteristics, thus avoiding any need to rely on theoretical modelling of the background.

A typical high- E_T photon candidate consists of signals from a cluster of 4–5 BEMC cells. Two shape-dependent quantities were used to distinguish γ , π^0 and η signals [5]. These were (i) the mean width $\langle\delta Z\rangle$ of the cell cluster in Z , which is the direction of finer segmentation of the BEMC, and (ii) the fraction f_{max} of the cluster energy found in the most energetic cell in the cluster. The quantity $\langle\delta Z\rangle$ is defined as $\sum (E_{cell}|Z_{cell} - \bar{Z}|) / \sum E_{cell}$, summing over the cells in the cluster, where \bar{Z} is the energy-weighted mean Z value of the cells. The $\langle\delta Z\rangle$ distribution for the event sample is shown in Figure 1(a), in which peaks due to the photon and π^0 contributions are clearly visible.³ The Monte Carlo samples of single γ , π^0 and η were used to establish a cut on $\langle\delta Z\rangle$ at 0.65 BEMC cell widths, such as to remove most of the η mesons but few of the photons and π^0 s. Candidates with lower $\langle\delta Z\rangle$ were retained, thus providing a sample that consisted of photons, π^0 mesons and a small admixture of η mesons.

The extraction of the photon signal from the mixture of photons and a neutral meson background was done by means of the f_{max} distributions. Figure 1(b) shows the shape of the f_{max} distribution for the final event sample, after the $\langle\delta Z\rangle$ cut, fitted to the η component determined from the $\langle\delta Z\rangle$ distribution plus freely-varying γ and π^0 contributions. Above an f_{max} value of 0.75, the distribution is dominated by the photons; below this value it consists mainly of meson background. Since the shape of the f_{max} distribution is similar for the η and π^0 contributions, the background subtraction is insensitive to uncertainties in the fitted π^0 to η ratio.

The numbers of candidates with $f_{max} > 0.75$ and $f_{max} < 0.75$ were calculated for the sample of events occurring in each bin of a measured quantity. From these numbers, and the ratios of the corresponding numbers for the f_{max} distributions of the single particle samples, the number of photon events in the given bin was evaluated [5].

6 Cross section calculation and systematic uncertainties

Cross sections are given for the photoproduction process $ep \rightarrow \gamma(\text{prompt}) + X$, taking place in the incident γp centre-of-mass energy (W) range 134–285 GeV, i.e. $0.2 < y < 0.9$. The virtuality of the incident photon is restricted to the range $Q^2 \lesssim 1 \text{ GeV}^2$, with a median value of approximately 10^{-3} GeV^2 . The cross sections represent numbers of events within a given bin, divided by the bin width and integrated luminosity. They are given at the hadron level, with an isolation cone defined around the prompt photon

³The displacement of the photon peak from the Monte Carlo prediction does not affect the present analysis; the poor fit in the region $\langle\delta Z\rangle = 0.6\text{--}1.0$ is taken into account in the systematic errors.

as at the detector level. To obtain the hadron-level cross sections, bin-by-bin correction factors were applied to the corresponding detector-level distributions; these factors were calculated using PYTHIA.

The following sources of systematic error were taken into account:

1. *Calorimeter simulation*: the uncertainty of the simulation of the calorimeter response [15] gives rise to an uncertainty on the cross sections of $\pm 7\%$;
2. *Modelling of the shower shape*: uncertainties on the agreement of the simulated f_{max} distributions with the data correspond to a systematic error averaging $\pm 8\%$ on the final cross sections;
3. *Kinematic cuts*: the cuts defining the accepted kinematic range at the detector level were varied by amounts corresponding to the resolution on the variables. Changes of up to 5% in the cross section were observed;
4. $\eta/(\eta + \pi^0)$ *ratio*: the fitted value was typically 25%; variations of this ratio in the range 15–35% led to cross section variations of around $\pm 2\%$;
5. *Vertex cuts*: narrowing the vertex cuts to $(-25, +15)$ cm from their standard values of $(-50, +40)$ cm gave changes in the cross sections of typically $\pm 4\%$.

In addition, studies were made of the effects of using HERWIG instead of PYTHIA for the correction factors, of varying the E_T distribution applied to the single-particle samples, and of varying the composition of the Monte Carlo simulation in terms of direct, resolved and radiative processes. These gave changes in the cross sections at the 1% level. The 1.6% uncertainty on the integrated luminosity was neglected. The individual contributions were combined in quadrature to give the total systematic error.

7 Theoretical calculations

In presenting cross sections, comparison is made with two types of theoretical calculation, in which the pdf sets taken for both the photon and proton can be varied, although there is little sensitivity to the choice of proton pdf. These are:

(i) PYTHIA and HERWIG calculations evaluated at the final-state hadron level, as outlined in Sect. 4. Each of these programs comprises a set of LO matrix elements augmented by parton showers in the initial and final states together with hadronisation;

(ii) NLO parton-level calculations of Gordon (LG) [16, 17] and of Krawczyk and Zembruski (K&Z) [18]. Pointlike and hadronic diagrams at the Born level are included, together with virtual (loop) corrections and terms taking into account three-body final states. The radiative terms are evaluated by means of fragmentation functions obtained from experiment. In both calculations, the isolation criterion was applied at the parton level.

The LG and K&Z calculations differ in several respects [16–19]. The K&Z calculation includes a box-diagram contribution for the process $\gamma g \rightarrow \gamma g$ [20], but excludes higher-order corrections to the resolved terms which are present in LG. A value of $\Lambda_{\overline{MS}} = 200$

MeV (5 flavours) is used in LG while in K&Z a value of 320 MeV (4 flavours) is used, so as to reproduce a fixed value of $\alpha_S = 0.118$ at the Z^0 mass. The standard versions of both calculations use a QCD scale of p_T^2 . Both calculations use higher-order (HO) versions of the GRV [14] and GS [21] photon pdf sets.

8 Results

Figure 2 and Table 1 give the inclusive cross-section $d\sigma/dE_T^\gamma$ for the production of isolated prompt photons in the range $-0.7 < \eta^\gamma < 0.9$ for $0.2 < y < 0.9$. All the theoretical models describe the shape of the data well; however the predictions of PYTHIA and especially HERWIG are too low in magnitude. The LG and K&Z calculations give better agreement with the data.

Figure 3 and Table 2 give the inclusive cross-section $d\sigma/d\eta^\gamma$ for isolated prompt photons in the range $5 < E_T^\gamma < 10$ GeV for $0.2 < y < 0.9$. Using the GRV pdf's in the photon, PYTHIA gives a good description of the data for forward pseudorapidities. The HERWIG distribution, while similar in shape to that of PYTHIA, is lower throughout; this is attributable chiefly to the lower value of the radiative contribution in HERWIG (see Sect. 4). The LG and K&Z calculations using GRV are similar to each other and to PYTHIA. All the calculations lie below the data in the lower η^γ range.

The effects were investigated of varying some of the parameters of the K&Z calculation relative to their standard values (NLO, 4 flavours, $\Lambda_{\overline{MS}} = 320$ MeV, GRV photon pdf). Reducing the number of flavours used in the calculation to three (with $\Lambda_{\overline{MS}} = 365$ MeV) reduced the cross sections by 35–40% across the η^γ range, confirming the need to take charm into account. A LO calculation (with $\Lambda_{\overline{MS}} = 120$ MeV and a NLO radiative contribution) was approximately 25% lower than the standard NLO calculation. Variations of the QCD scale between $0.25E_T^2$ and $4E_T^2$ gave cross-section variations of approximately $\pm 3\%$.

Figure 3(b) illustrates the effects of varying the photon parton densities, comparing the results using GRV with those using GS. The ACFGP parton set [22] gives results (not shown) similar to GRV. All NLO calculations describe the data well for $\eta^\gamma > 0.1$, as does PYTHIA, but are low at more negative η^γ values, where the curves using the GS parton densities give poorer agreement than those using GRV.

As a check on the above results, the same cross sections were evaluated with the additional requirement that each event should contain a jet (see [5]) with $E_T \geq 5$ GeV in the pseudorapidity range $(-1.5, 1.8)$. Both the measured and theoretical distributions were found to be of a similar shape to those in Fig. 3.

The discrepancy between data and theory at negative η^γ is found to be relatively strongest at low values of y . Figure 4 shows the inclusive cross section $d\sigma/d\eta^\gamma$ as in Fig. 3, evaluated for the three y ranges 0.2–0.32, 0.32–0.5 and 0.5–0.9 by selecting the y^{meas} ranges 0.15–0.25, 0.25–0.4 and 0.4–0.7 at the detector level. The numerical values are listed in Table 2. In the lowest y range, both theory and data show a peaking at negative η^γ , but it is stronger in the data. The Monte Carlo calculations indicate that the peak occurs at more

negative η^γ values as y increases, eventually leaving the measurement acceptance. In the highest y range (Fig. 4(c)), agreement is found between theory and data. The movement of the peak can be qualitatively understood by noting that for fixed values of E_T and x_γ , where x_γ is the fraction of the incident photon energy that contributes to the resolved QCD subprocesses, measurements at increasing y correspond on average to decreasing values of pseudorapidity. By varying the theoretical parameters, the discrepancy was found to correspond in the K&Z calculation to insufficient high x_γ partons in the resolved photon.

9 Summary and conclusions

The photoproduction of isolated prompt photons within the kinematic range $0.2 < y < 0.9$, equivalent to incident γp centre-of-mass energies W of 134–285 GeV, has been measured in the ZEUS detector at HERA, using an integrated luminosity of 38.4 pb^{-1} . Inclusive cross sections for $ep \rightarrow \gamma + X$ have been presented as a function of E_T^γ for photons in the pseudorapidity range $-0.7 < \eta^\gamma < 0.9$, and as a function of η^γ for photons with $5 < E_T^\gamma < 10 \text{ GeV}$. The latter results have been given also for three subdivisions of the y range. All kinematic quantities are quoted in the laboratory frame.

Comparisons have been made with predictions from leading-logarithm parton-shower Monte Carlo (PYTHIA and HERWIG), and from next-to-leading-order parton-level calculations. The models are able to describe the data well for forward (proton direction) photon pseudorapidities, but are low in the rear direction. None of the available variations of the model parameters was found to be capable of removing the discrepancy with the data. The disagreement is strongest in the W interval 134–170 GeV, but not seen within the measurement acceptance for $W > 212 \text{ GeV}$. This result, together with the disagreements with NLO predictions seen also in recent dijet results at HERA [4], would appear to indicate a need to review the present theoretical modelling of the parton structure of the photon.

Acknowledgements

It a pleasure to thank the DESY directorate and staff for their unfailing support and encouragement. The outstanding efforts of the HERA machine group in providing high luminosity for the 1996–97 running are much appreciated. We are also extremely grateful to L. E. Gordon, M. Krawczyk and A. Zembruski for helpful conversations, and for making available to us calculations of the NLO prompt photon cross section and a computer program (K&Z).

References

- [1] ZEUS Collab., M. Derrick et al., Phys. Lett. **B322** (1994) 287;
ZEUS Collab., M. Derrick et al., Phys. Lett. **B348** (1995) 665;
ZEUS Collab., M. Derrick et al., Phys. Lett. **B384** (1996) 401.
- [2] H1 Collab., T. Ahmed et al., Phys. Lett. **B297** (1992) 205;
H1 Collab., T. Abt et al., Phys. Lett. **B314** (1993) 436;
H1 Collab., T. Ahmed et al., Nucl. Phys. **B445** (1995) 195;
H1 Collab., S. Aid et al., Phys. Lett. **B392** (1997) 234.
- [3] ZEUS Collab., J. Breitweg et al., Eur. Phys. J. **C4** (1998) 591.
- [4] ZEUS Collab., J. Breitweg et al., Eur. Phys. J. **C1** (1998) 109;
ZEUS Collab., J. Breitweg et al., DESY 99-057, to appear in Eur. Phys. J.
- [5] ZEUS Collab., J. Breitweg et al., Phys. Lett. **B413** (1997) 201.
- [6] ZEUS Collab., M. Derrick et al., Phys. Lett. **B297** (1992) 404.
- [7] A. Andresen et al., Nucl. Instr. Meth. **A309** (1991) 101;
A. Bernstein et al., Nucl. Instr. Meth. **A338** (1993) 23;
A. Caldwell et al., Nucl. Instr. Meth. **A321** (1992) 356.
- [8] N. Harnew et al., Nucl. Instr. Meth. **A279** (1989) 290;
B. Foster et al., Nucl. Phys. **B** (Proc. Suppl.) **32** (1993) 181; Nucl. Instr. Meth. **A338** (1994) 254.
- [9] ZEUS Collab., M. Derrick et al., Z. Phys. **C65** (1995) 379.
- [10] R. Brun et al., CERN-DD/EE/84-1 (1987).
- [11] H.-U. Bengtsson and T. Sjöstrand, Comp. Phys. Commun. **46** (1987) 43;
T. Sjöstrand, CERN-TH.6488/92.
- [12] G. Marchesini et al., Comp. Phys. Commun. **67** (1992) 465.
- [13] A. D. Martin, R. G. Roberts and W. J. Stirling, Phys. Rev. **D50** (1994) 6734.
- [14] M. Glück, E. Reya and A. Vogt, Phys. Rev. **D46** (1992) 1973.
- [15] ZEUS Collab., J. Breitweg et al., Eur. Phys. J. **C6** (1999) 67;
ZEUS Collab., M. Derrick et al., Z. Phys. **C72** (1996) 399.
- [16] L. E. Gordon, Phys. Rev. **D57** (1998) 235 and private communication;
L. E. Gordon, hep-ph/9706355 and Proceedings, *Photon 97*, Egmond aan Zee, eds.
A. Buijs and F. Ern  (World Scientific, Singapore, 1998), 173.
- [17] L. E. Gordon and W. Vogelsang, hep-ph/9606457 and Proceedings, *DIS96*, Rome,
eds. G. D'Agostini and A. Nigro, (World Scientific, Singapore, 1997), 278.

- [18] M. Krawczyk and A. Zembrzuski, [hep-ph/9810253](#) and Proceedings, *Photon 97*, Egmond aan Zee, eds. A. Buijs and F. Ern e (World Scientific, Singapore, 1998), 162 and private communication.
- [19] M. Klasen, [hep-ph/9907366](#).
- [20] B. L. Combridge, *Nucl. Phys.* **B174** (1980) 243.
- [21] L. E. Gordon and J. K. Storrow, *Nucl. Phys.* **B489** (1997) 405.
- [22] P. Aurenche et al., LPTHE preprint 92/13;
P. Aurenche et al., *Z. Phys.* **C64** (1994) 621.

E_T^γ	$d\sigma/dE_T^\gamma$ pb GeV ⁻¹
5.0 - 6.0	18.4 ± 2.1 $^{+2.6}_{-2.8}$
6.0 - 7.0	9.9 ± 1.3 $^{+1.2}_{-1.3}$
7.0 - 8.0	8.7 ± 1.1 $^{+0.9}_{-0.7}$
8.0 - 9.5	3.3 ± 0.6 $^{+0.4}_{-0.5}$
9.5 - 11.0	2.2 ± 0.4 $^{+0.2}_{-0.3}$
11.0 - 13.0	1.3 ± 0.3 $^{+0.2}_{-0.2}$
13.0 - 15.0	0.3 ± 0.3 $^{+0.2}_{-0.1}$

Table 1: Differential cross sections for inclusive photoproduction of isolated photons with $-0.7 < \eta^\gamma < 0.9$, averaged over given transverse-energy intervals, for $0.2 < y < 0.9$ ($134 < W < 285$ GeV). The first error is statistical, the second is systematic.

η^γ	$d\sigma/d\eta^\gamma$ pb			
	$0.2 < y < 0.9$	$0.2 < y < 0.32$	$0.32 < y < 0.5$	$0.5 < y < 0.9$
	$134 < W < 285$	$134 < W < 170$	$170 < W < 212$	$212 < W < 285$
-0.6	38.9 ± 5.9 $^{+4.3}_{-4.7}$	10.0 ± 3.3 $^{+1.8}_{-2.2}$	15.2 ± 3.6 $^{+2.4}_{-2.5}$	13.7 ± 3.2 $^{+2.3}_{-3.1}$
-0.4	40.1 ± 5.7 $^{+4.3}_{-5.1}$	17.0 ± 3.6 $^{+3.1}_{-1.9}$	13.8 ± 3.2 $^{+2.1}_{-2.7}$	9.3 ± 2.8 $^{+1.5}_{-2.2}$
-0.2	27.7 ± 5.0 $^{+2.8}_{-4.1}$	11.4 ± 3.1 $^{+2.1}_{-2.2}$	11.7 ± 2.9 $^{+1.9}_{-2.0}$	4.6 ± 2.1 $^{+0.7}_{-1.3}$
0.0	35.1 ± 5.5 $^{+4.1}_{-3.6}$	17.7 ± 3.5 $^{+3.1}_{-2.2}$	9.1 ± 3.0 $^{+1.7}_{-1.6}$	8.3 ± 2.7 $^{+1.3}_{-1.9}$
0.2	21.0 ± 4.4 $^{+3.3}_{-3.0}$	9.9 ± 2.5 $^{+2.1}_{-1.8}$	5.7 ± 2.4 $^{+1.2}_{-1.1}$	5.4 ± 2.4 $^{+1.1}_{-1.4}$
0.4	18.7 ± 3.7 $^{+2.1}_{-2.2}$	7.2 ± 2.1 $^{+1.4}_{-0.9}$	7.9 ± 2.4 $^{+1.4}_{-1.6}$	3.6 ± 1.7 $^{+0.6}_{-0.9}$
0.6	14.4 ± 4.4 $^{+2.1}_{-2.3}$	6.8 ± 2.7 $^{+1.4}_{-1.0}$	5.8 ± 2.5 $^{+0.9}_{-1.3}$	1.8 ± 2.2 $^{+0.6}_{-0.7}$
0.8	19.5 ± 4.9 $^{+2.1}_{-2.6}$	6.8 ± 2.9 $^{+1.3}_{-1.3}$	10.1 ± 3.4 $^{+2.3}_{-1.5}$	2.6 ± 2.2 $^{+0.5}_{-0.9}$

Table 2: Differential cross sections per unit pseudorapidity for inclusive photoproduction of isolated photons with $5 < E_T^\gamma < 10$ GeV, averaged over laboratory pseudorapidity intervals of ± 0.1 about the given central values. The γp centre-of-mass energy (W) ranges are in GeV. Results are listed for the full range of fractional incident photon energy y and in three subdivisions. The first error is statistical, the second is systematic.

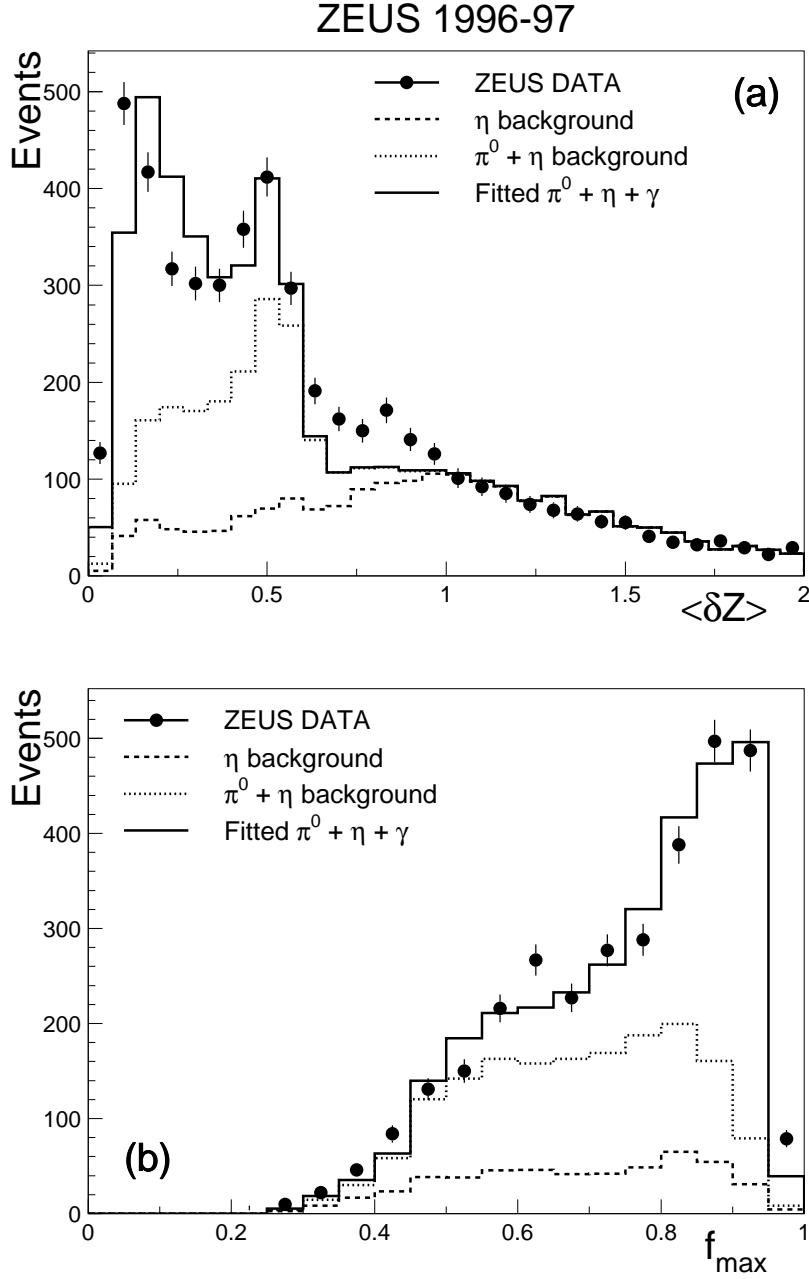


Figure 1: (a) Distribution of $\langle \delta Z \rangle$ for prompt photon candidates in selected events. (b) Distribution of f_{max} for prompt photon candidates in selected events after cutting on $\langle \delta Z \rangle$. Also given in both cases are fitted Monte Carlo distributions for photons, π^0 and η mesons with similar selection requirements as for the observed photon candidates. Samples with $f_{max} > 0.75$ and $f_{max} < 0.75$ are enriched in the photon signal and in the meson background, respectively.

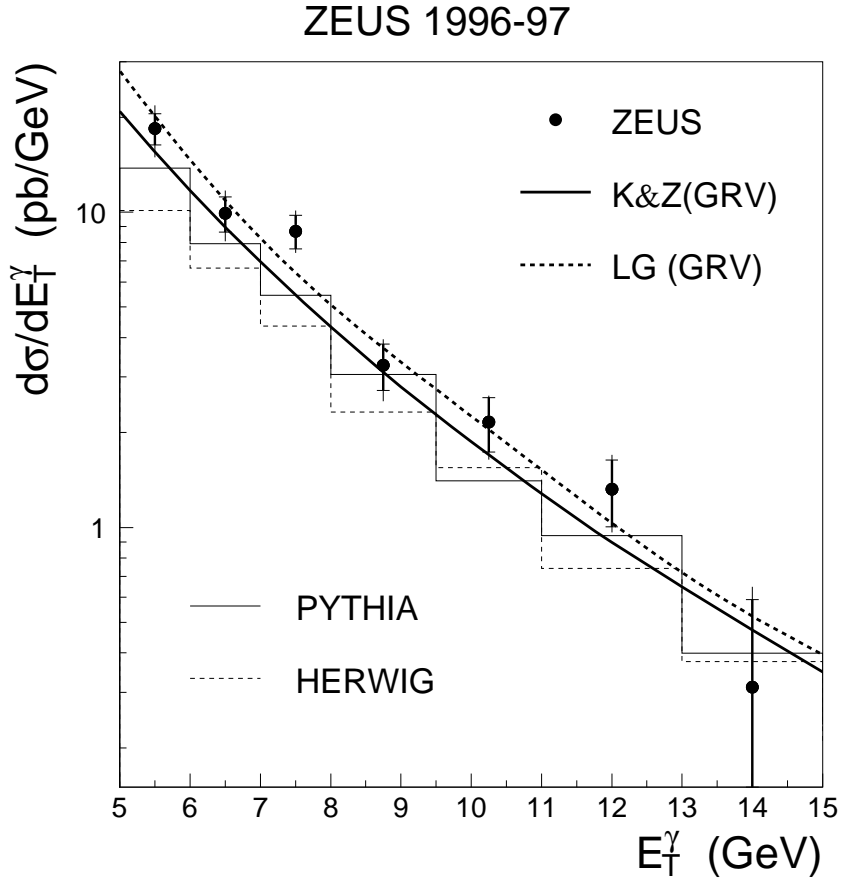


Figure 2: Differential cross section $d\sigma/dE_T^\gamma$ for prompt photons produced over $-0.7 < \eta^\gamma < 0.9$. The inner (thick) error bars are statistical; the outer include systematic errors added in quadrature. The data points are plotted at the respective bin centres (see Table 1; bin centring corrections are negligible). Predictions are shown from PYTHIA and HERWIG at the hadron level (histograms), and from LG and K&Z (curves). In K&Z, the default 4-flavour NLO $\Lambda_{\overline{MS}}$ value of 320 MeV is used.

ZEUS 1996-97

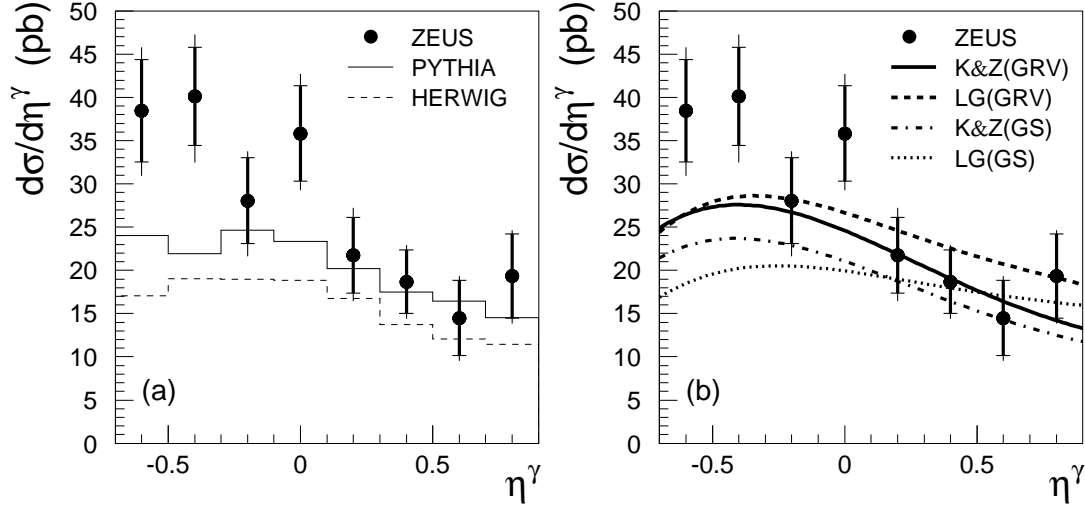


Figure 3: Differential cross-section $d\sigma/d\eta^\gamma$ for isolated prompt photons with $5 < E_T^\gamma < 10$ GeV, for $0.2 < y < 0.9$ ($134 < W < 285$ GeV). The inner (thick) error bars are statistical; the outer include systematic errors added in quadrature. Also plotted are (a) PYTHIA and HERWIG predictions using the GRV(LO) photon parton densities; (b) LG and K&Z NLO predictions using GRV(HO) and GS(HO) photon parton densities.

ZEUS 1996-97

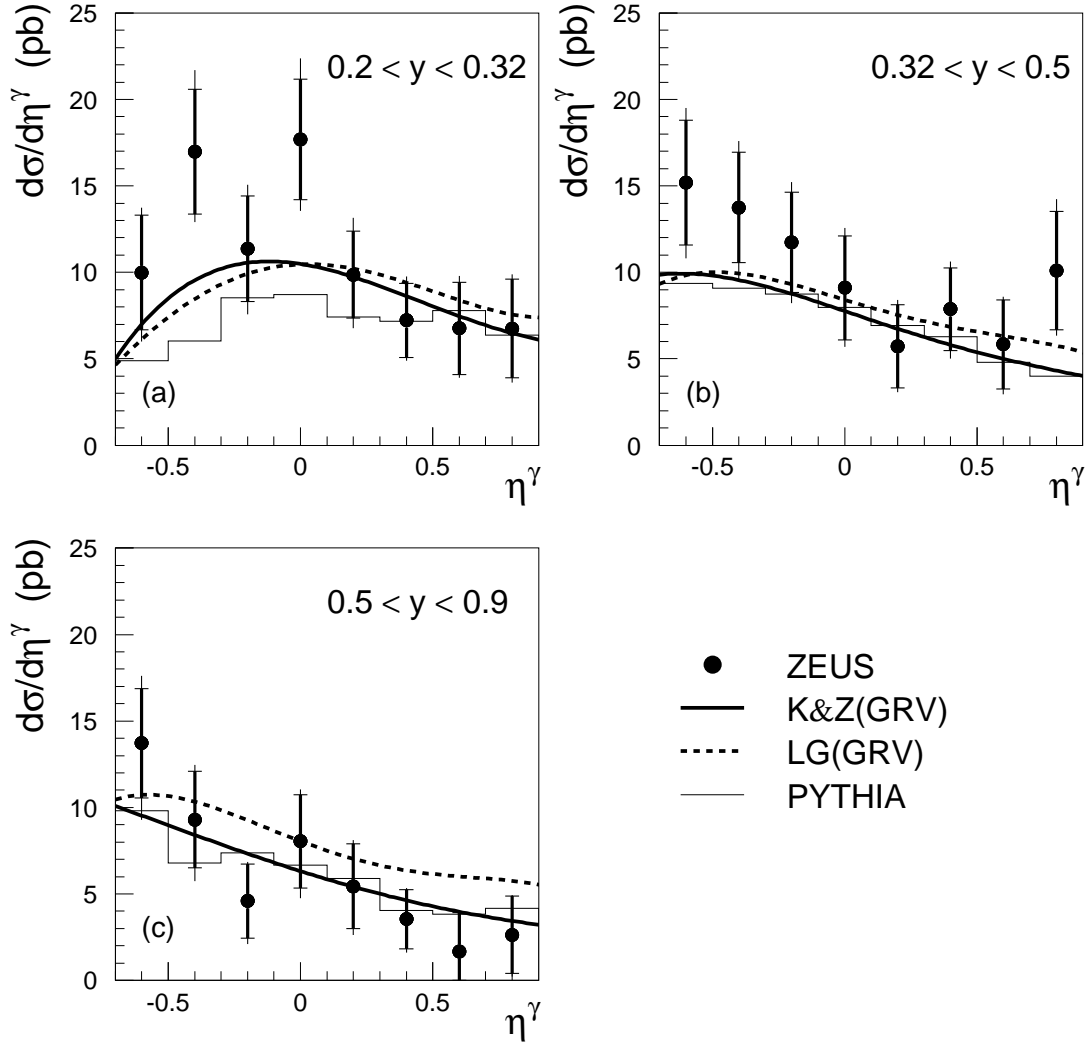


Figure 4: Differential cross-section $d\sigma/d\eta^\gamma$, for isolated prompt photons with $5 < E_T^\gamma < 10$ GeV, compared with PYTHIA and with LG and K&Z NLO predictions, using GRV photon parton densities as in Fig. 3. The inner (thick) error bars are statistical; the outer include systematic errors added in quadrature. The plots correspond to the W ranges (a) 134–170 GeV, (b) 170–212 GeV, (c) 212–285 GeV.